Stability and Kinetics of Degradation of Imipenem in Aqueous Solution

GEORGE B. SMITH[x], GEORGE C. DEZENY, AND ALAN W. DOUGLAS

Received July 21, 1989, from *Merck, Sharp and Dohme Research Laboratories, Rahway, NJ 07065.*
Accepted for publication November 8, 1989.

Abstract □ In weakly acidic solution, the broad-spectrum antibiotic imipenem undergoes complex oligomerization initiated by intermolecular carboxyl group attack on the β-lactam group. In weakly alkaline solution, intermolecular reaction between the β-lactam and formimidoyl groups occurs instead. Both β-lactam and formimidoyl groups also hydrolyze at pH-dependent rates. Complex decomposition schemes were determined in kinetic studies at pH 4.0 and 9.0–9.5 using HPLC and mathematical models. The rates of the several initial reactions, calculated as functions of pH and imipenem concentration by fitting the models to kinetic data, fully account for imipenem decomposition rates throughout the neutral pH range.

Imipenem (**1**) is an important broad-spectrum β-lactam antibiotic which is both produced and administered in aqueous solution. Its stability in nonnucleophilic inert buffers from pH 5 to 8 at 25 and 40 °C, as determined using UV spectroscopy to measure intact β-lactam, has been reported.[1] The study revealed that rate-determining β-lactam opening precedes the formation of several products whose structures were not established. Pseudo first-order β-lactam hydrolysis was observed in dilute aqueous solutions of **1** (1 and 2 mg/mL), and faster decomposition at higher concentrations was ascribed to undefined parallel second-order reactions of **1** with itself.

The purpose of the present study was to gain a comprehensive understanding of the nonoxidative decomposition of **1** in the neutral pH range, by identifying the products and measuring their reaction rates. Decomposition was shown to involve reactions of certain functional groups. Reaction mixtures soon became quite complex since those groups were present both in **1** and its products. Even greater complexity due to air oxidation was avoided by keeping the mixtures under nitrogen.

Different reactions prevail in weakly acidic and weakly alkaline solutions. In the former, decomposition of **1** is initiated mainly by β-lactam hydrolysis and intermolecular reaction of β-lactam and protonated carboxylic acid groups. In the latter, decomposition begins with hydrolyses of the β-lactam and formimidoyl groups and intermolecular reaction of β-lactam and unprotonated formimidoyl groups. The complex decomposition in the neutral pH range, involving all of these reactions, was elucidated in separate HPLC kinetic studies at pH 4.0 and 9.0–9.5. The decomposition rates at these particular pH values were convenient experimentally. Chromatographically observed decomposition products were isolated using analytical or semipreparative HPLC and were identified spectroscopically. Kinetic models developed concurrently were used for determination of reaction rate expressions, evaluation of reactivities, and visualization of the decomposition.

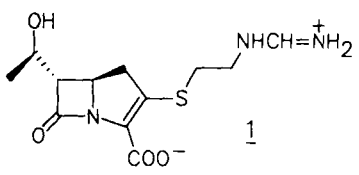

1

In the previous study[1] at pH 5 to 8, the β-lactam reaction of **1** in dilute solution was shown to be pseudo first order with rate dependence on pH consistent with the following equation:

$$k_{pH} = k_H a_H + k_o + k_{OH}(K_W/a_H) \quad (1)$$

where k_{pH} is the apparent first-order rate constant at a given pH, k_H and k_{OH} are the rate constants for hydrogen ion-catalyzed and hydroxide ion-catalyzed hydrolyses, respectively, k_o is the rate constant for spontaneous degradation, K_W is the dissociation constant of water, and a_H is the hydrogen ion activity as measured by the glass electrode. The nonnucleophilic MES and MOPS buffers (see *Experimental Section*) used as solvents were found inert in that reaction rates were independent of buffer concentration up to 1 M. In runs not reported previously, the rate effect of ionic strength was found negligible; that is, reaction rates were unchanged by sodium chloride up to a concentration of 0.5 M.

An undefined intermolecular second-order reaction competing with the pseudo first-order β-lactam hydrolysis was proposed to account for the faster loss of the β-lactam group observed at higher concentration. Subsequently, involvement of the carboxylic acid group and/or the basic side chain in intermolecular reaction with the β-lactam group was suspected. Stability studies carried out with sodium acetate and 2-methoxyethylamine as model compounds confirmed these hypotheses as follows.

Dilute solutions of **1** with sodium acetate or the amine in large excess, buffered in the neutral pH range, were analyzed periodically for intact β-lactam. Pseudo first-order β-lactam disappearance was observed, with apparent reactivities proportional to the molarity of model compound at a given pH. The apparent reactivity with sodium acetate varied with pH in proportion to the concentration of protonated acetic acid, calculated from its pK_a value of 4.75.[2] That with 2-methoxyethylamine varied in proportion to the concentration of unprotonated amino group (pK_a = 9.45[3]). Thus, the protonated carboxyl and unprotonated formimidoyl groups of **1** were implicated in the intermolecular β-lactam reaction.

Unbuffered aqueous solutions of **1** were used in kinetic runs at pH 4.0, 9.0, and 9.5 described herein. Since **1** has pK_a values of 3.2 and 9.9,[1] it exists largely as the zwitterion (shown above) between pH 4 and 9.5. Furthermore, the formimidoyl group exists as interconverting *Z*- and *E*-formamidinium isomers due to hindered rotation about the NC partial double bond.[4] For the sake of clarity, charges and formamidinium isomers are not included in the following schemes.

0022-3549/90/0800-0732$01.00/0

Acid-Catalyzed Decomposition Pathways—An important finding related to the second-order decomposition of **1** in acidic solution was revealed when its *S*-methyl analogue was treated at pH 3 with sulfuric acid. Diketopiperazine dimer **4b** was the predominant product, which precipitated from the aqueous solution.[4]

Diketopiperazine **4a** (Scheme I) was proposed[4] as a major degradate of aqueous **1** at pH 4.5 and a concentration of 20–30 mg/mL; **4a** formed in greater yield at higher concentration. The ^{13}C NMR data for **4a** and **4b** were quite similar.

Among the several pH 4 degradates of **1** observed using HPLC in the present kinetic study, only **3** appeared initially. Formation of dimers **3** and **4a** by consecutive intermolecular and intramolecular reactions of β-lactam and carboxylic acid groups is depicted in Scheme I. The formation of **3** and **4a** from **1** was also followed using FTIR. Separate bands were assigned to the amidic carbonyls of **3** and **4a** and to the combined β-lactam carbonyls of **1** and **3**. By subtracting the contributions of **1** from spectra of the reaction mixture, **3** was shown to have the same formimidoyl intensity but only half of the β-lactam intensity of **1**. The concentration of **3** increased initially, peaked, and then decreased as **4a** formed (see *Kinetics of Decomposition in Weakly Acidic Solutions* below).

Structures **5**, **6**, and **7**, deduced as products of comparable

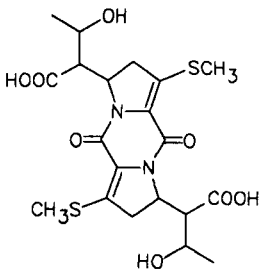

4b

intermolecular and intramolecular reactions of β-lactam and carboxylic acid groups, were assigned to the other HPLC peaks observed in kinetic runs at pH 4 in the absence of air (Scheme II). (Many more peaks appeared if air was not excluded.) Trimer **5** probably formed from **3**, and **6** from **4a**, by intermolecular reactions of the aliphatic carboxylic acids with the β-lactam of **1**. Further, we assumed that diketopiperazine **6** formed from **5**, and **4a** from **3**, by intramolecular reactions of the ring acids, and that diketoperhydrodiazepin **7** formed from **3** by intramolecular reaction of the aliphatic acid. Compound **7** was isolated chromatographically, and its structure was confirmed using NMR (see *Experimental Section*).

The other possible product of **1** and **3**, not shown in Scheme II, is the trimer formed both by reaction of the **3** ring acid and the **1** β-lactam group and of the **1** (ring) acid and the **3** β-lactam group. This trimer was not observed, and its theoretical yield, based on the model, was lower than those of the observed degradates.

The assignments were consistent with HPLC kinetic data (see below), relative retention times, and peak absorbance

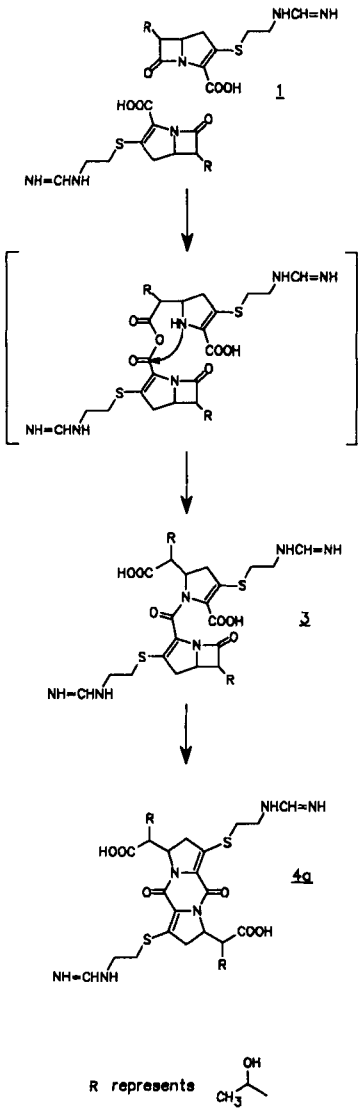

Scheme I

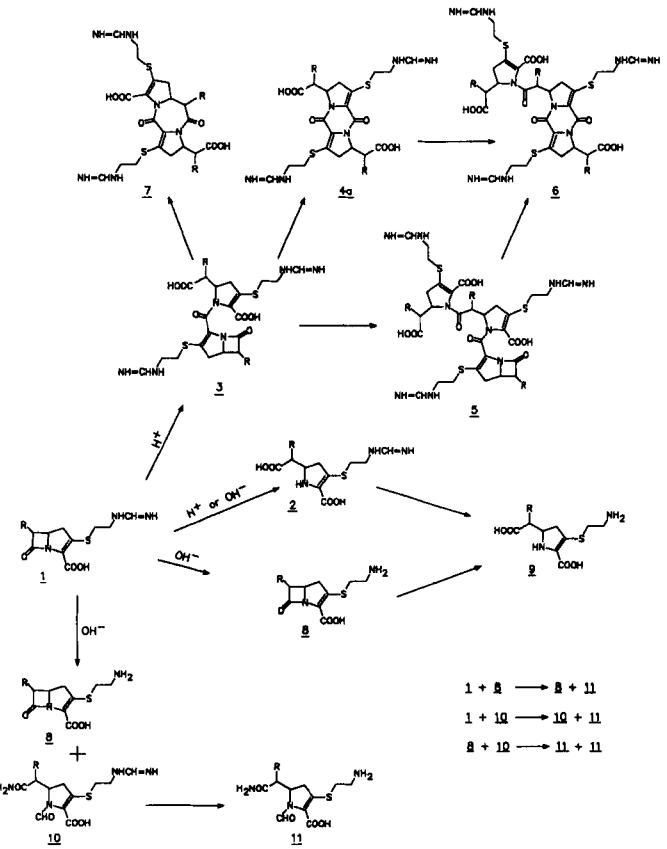

Scheme II

wavelengths measured using a diode array detector (Table I and Figure 3). The retention times of **4a** and **6** were somewhat shorter than those of their respective precursors, **3** and **5**. Both diketopiperazines **4a** and **6** exhibited absorbance peaks at 360 nm, and an additional peak of the latter at lower wavelength seemed to be due to the pendant enamidic unit of the trimer. The absorbance spectrum of **5** was uncertain because its HPLC peaks were relatively small and broad at long retention times. These assignments were confirmed using sulfuric acid as a reagent to cleave β-lactams. When pH 4 reaction mixtures were treated with sulfuric acid, **1**, **3**, and **5** disappeared rapidly, while **4a**, **6**, and **7** remained.

Base-Catalyzed Decomposition Pathways—Thienamycin **8**, an imipenem impurity, was recognized by its retention time and UV spectrum using authentic reference material.[5] Its appearance as the product of formimidoyl group hydrolysis in dilute solution of **1** at pH 9.5 was obvious. Faster decomposition of **1** at higher concentration at pH 9.0–9.5 was accompanied by appearance of both **8** and **10**, a dihydropyrrole whose formation from 2 mol of **1** via an unstable dimer is depicted in Scheme III. Compound **10** was the major reaction product (and ammonia the assumed byproduct) of **1** and excess formamidine under similar conditions. It was isolated chromatographically from aged solutions of imipenem with or without formamidine (see *Experimental Section*) and identified using NMR, FTIR, and MS.

The identity of **10** was confirmed by spectroscopic observations of the acid hydrolysis of its N-formyl group ($t_{1/2}$ ~1 h at room temperature in 1 M aqueous DCl). The UV and NMR spectra, recorded periodically, indicated concurrent disappearance of **10** and appearance of a product similar to the β-lactam hydrolysis product **2**, described by Ratcliffe et al.[4] The NMR spectra included the signal of the formic acid byproduct.

In similar reactions of the same functional groups, attacks by the formimidoyl group of **1** on the β-lactam group of **8** and by that of **10** on the β-lactam groups of **1** and **8** would produce **8**, **10**, and **11**, as noted in Scheme II. Formimidoyl group hydrolysis of **10** would produce **11**, also. The HPLC peaks of the carbapenems **1** and **8** exhibited UV spectra with absorbance maxima at higher wavelengths than those assigned to the dihydropyrroles **10** and **11** (Table II and Figure 2), and the dihydropyrroles were much more stable toward hydroxylamine.

Intermolecular reactions involving attack by amino groups on β-lactam groups were known to produce oligomers. An initial degradate of aqueous **8** was characterized as a dimer formed upon intermolecular aminolysis of its β-lactam group and retaining half of the β-lactam absorbance of the starting material.[5] In the present study at pH 9.0–9.5, HPLC degradate peaks other than those of **1**, **8**, **10**, and **11** were very minor peaks (amounting to ~0.1% of the initial **1** peak area) at longer retention times and possibly included dimers formed by reactions of the amino groups of **8**, **9**, and **11** with the β-lactam groups of **1** and **8**.

Kinetic modeling was essential to enlightened interpretation of the multivariate HPLC data obtained in the separate kinetic studies at pH 4.0 and 9.0–9.5. The models included **1**, its degradates whose concentrations were measured using HPLC, and unmeasured degradates whose concentrations were defined implicitly (i.e., calculable from the HPLC data within the framework of the model). Model construction and fitting to the kinetic data are described below. Plots versus reaction time summarize calculated concentrations, both explicit and implicit, and show reasonable agreement of the former with the data.

Table I—Correlation of pH 4 HPLC Peaks, Structures, and UV Spectra

Retention Time, min	Structure (Scheme II)	Absorbance λ_{max}, nm
6	**1**	300
9	**4a**	360
12	**3**	285
16	**7**	330
19	**6**	360, 280
26	**5**	—

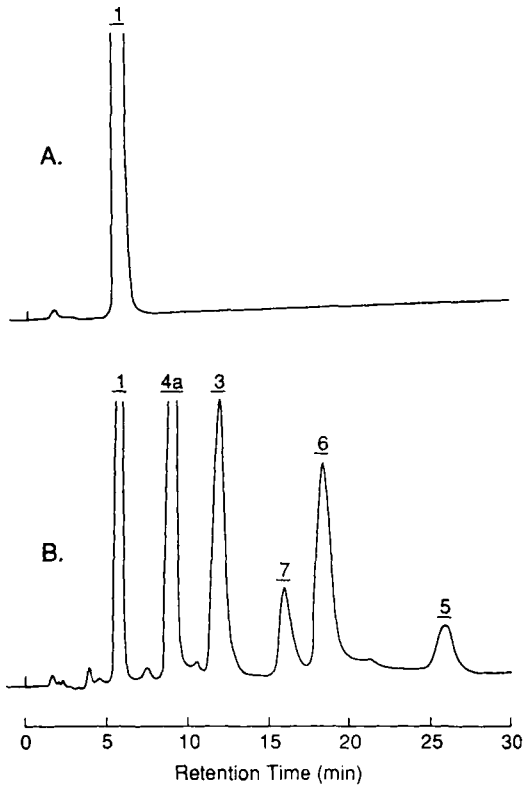

Figure 1—Chromatograms of the pH 4 reaction mixture with initial **1** concentration of 20 mg/mL initially (**A**) and after 2 h at 20 °C (**B**).

Kinetics of Decomposition in Weakly Acidic Solution—Imipenem (**1**) in aqueous solution at pH 4 undergoes decomposition initiated by hydrolysis of its β-lactam group and parallel intermolecular reaction of its β-lactam and carboxylic acid groups, forming **2** and **3**, respectively (Scheme II). Hydrolysis of the formimidoyl group and intermolecular reaction of the β-lactam and formimidoyl groups, important at higher pH, are insignificant at pH 4. Also, the pH–stability profile of dilute **1** indicates that hydroxide ion-catalyzed hydrolysis and spontaneous degradation of the β-lactam group are insignificant compared with hydrogen ion-catalyzed hydrolysis at pH 4 (eq 1).

A kinetic model encompassing our understanding of the decomposition at pH ~4 was constructed of simultaneous differential equations describing the derivatives of the molarities of **1**–**7**, whose β-lactam groups participate (according to Scheme II) in the five types of reactions: pseudo first-order hydrogen ion-catalyzed hydrolysis, second-order intermolecular reactions with ring and aliphatic acids, and first-order intramolecular reactions with ring and aliphatic acids. At first, equal reactivities of like functional groups were assumed for each of these types.

The reactivity of **1** with sodium acetate was found proportional to the fraction of acetate protonated, existing as acetic acid. Thus the concentrations of the protonated forms of carboxylic acid reactants appeared in the rate expressions of

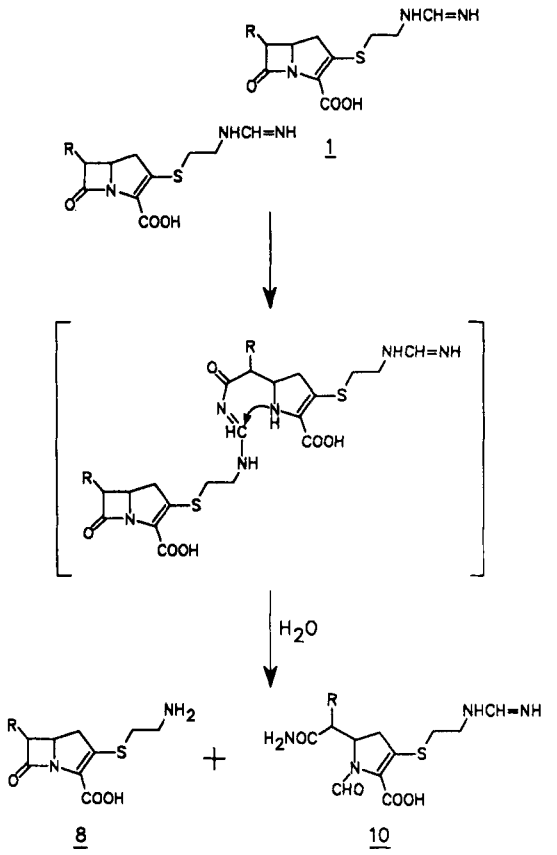

Scheme III

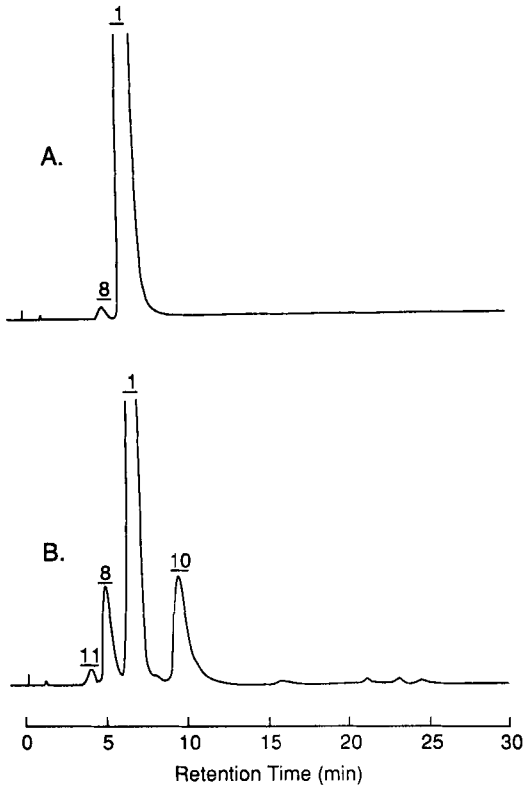

Figure 2—Chromatograms of the pH 9 reaction mixture with initial **1** concentration of 20 mg/mL (**A**) and after 4 h at 20 °C (**B**).

Table II—Correlation of pH 9 HPLC Peaks, Structures, and UV Spectra

Retention Time, min	Structure (Scheme II)	Absorbance λ_{max}, nm
4	**11**	288
5	**8**	298
7	**1**	300
9	**10**	290

the model. Fractions protonated were calculated using the pK_a values 3.2 of **1** for all ring acids and 4.6 of α-methyl-β-hydroxybutyric acid[6] for all aliphatic acids.

The kinetic data included HPLC peaks of **1** and **3–7** separated on a PAC column monitored at 320 nm, at which all of those peaks were measured with limits of detection of <0.1% of the initial **1** peak area. Kinetic data were not obtained for **2**, which eluted in broad bands with varying retention and absorbed only below 230 nm. Chromatograms of pH 4 reaction mixtures monitored at several wavelengths revealed no other peaks.

The model extended beyond the first, most important steps, shown in Scheme II to include the hydrolyses of the β-lactam groups of **3** and **5** and all possible intermolecular reactions of the β-lactam groups of **1**, **3**, and **5** with the carboxylic acid groups of **1–7**. Mole percent of initial **1** represented in a combined "pool" of all products other than **2–7** was calculated.

The model was fitted to data from two kinetic runs at pH 4.0 and 20 °C with initial **1** concentrations of 20 and 2 mg/mL, with sodium chloride in the reaction mixture of the latter run to make the ionic strengths equal. In another run at 2 mg/mL without sodium chloride, however, no ionic strength effect was evident. The simultaneous equations were integrated numerically to obtain the molarities M_1–M_7 and the "pool" content as functions of reaction time. A Gear integration method[7] was used and results were verified as unchanged when the tolerance parameter was varied. For comparison with the HPLC data, calculated mole percent yields of **3–7** were converted to area percent yields with response factors F_i, molar responses relative to that of **1** (eq 2). Both the rate constants and response factors were treated as parameters, adjusted using a simplex algorithm.[8] Integration and simplex parameter adjustment were iterated automatically until the aggregate sum of squared residuals of **1** and **3–7** of both runs was minimized.

$$\frac{100\ (\text{peak area})_i}{\text{initial 1 peak area}} = \frac{100\ M_i\ F_i}{\text{initial } M_1} \qquad (2)$$

The response factors of **4a**, **4b**, and **6** should be about the same since their chromophores are similar. When equal reactivities of like functional groups were assumed for each reaction type, however, the final calculated response factor of **4a** differed from that of **6** and from the known response factor of **4b**. These discrepancies were eliminated by assuming degradate β-lactam reactivities less than that of **1**, a possible result of steric hindrance. A multiplier denoted as Z was applied in the rate expressions both for the hydrolyses and intermolecular reactions of **3** and **5** and was included among the model parameters to be adjusted.

When the simplex iterative adjustment was carried out from various starting parameter values, the final calculated curves were found essentially invariant. Rate constants for **1** β-lactam hydrolysis and intermolecular reaction of the **1** β-lactam group and the **1** carboxylic acid were determined, since those final values were independent of the starting

Table III—Reactivities of Imipenem (1) at 20 °C

Decomposition Step	Reaction Step (Scheme II)	Rate Constant
Hydrogen ion-catalyzed 1 β-lactam hydrolysis	1→2	1400 $M^{-1} h^{-1}$ [a]
Intermolecular reaction of the 1 β-lactam and 1 protonated carboxylic acid	1→3	34 $M^{-1} h^{-1}$ [a]
Spontaneous 1 β-lactam degradation	1→2	0.0026 h^{-1} [b]
Hydroxide ion-catalyzed 1 β-lactam hydrolysis	1→2	10 000 $M^{-1} h^{-1}$ [c]
Hydroxide ion-catalyzed hydrolysis of the 1 unprotonated formimidoyl group	1→8	6000 $M^{-1} h^{-1}$ [c]
Intermolecular reaction of the 1 β-lactam and 1 unprotonated formimidoyl group	1 → 8 and 10	11 $M^{-1} h^{-1}$ [c]

[a] Obtained from kinetic data at pH 4. [b] Obtained from kinetic data at pH 5, 6, 7, and 8 with initial 1 concentration of 2 mg/mL. [c] Obtained from kinetic data at pH 9.0–9.5.

values (Table III). The other rate constants were found to be ambiguous; their final values depended on the starting values. The final Z value of 0.1 indicated reactivity of degradate β-lactam group (mainly the 3 β-lactam group) as being an order of magnitude lower than that of the 1 β-lactam group.

The results for the kinetic runs at pH 4.0 are plotted in Figures 3 and 4. The data and fitted concentration curves of 1 are shown in Figures 3A and 4A along with the corresponding calculated curves of 2 and the "pool", defined implicitly. The data and fitted curves of the explicit degradates are shown in Figures 3B and 4B. The ordinate of each curve is scaled to indicate the percentage of initial 1 represented; at any reaction time, the ordinate values of all the curves in Figure 3A and 3B, or 4A and 4B, are constrained to add up to 100%. At higher concentration, 1 decomposes faster, and the initial second-order reaction product 3, its further degradates, and the "pool" appear in larger amounts. At lower concentration, more pseudo first-order hydrolysis occurs.

According to the model, the calculated relative rates of formation of 4a and 7, formed by competitive ring closures involving the respective ring and aliphatic acid groups of 3, depend on the fractions protonated at a given pH. In imipenem decompositions at pH 3, 4, and 5, more 7 formed relative to 4a at higher pH, in agreement with the model.

Kinetics of Decomposition in Weakly Alkaline Solution—Imipenem (1) in aqueous solution at pH ~9 undergoes decomposition via three parallel reactions; that is, hydrolysis of the β-lactam moiety, hydrolysis of the *N*-formimidoyl group to an amino group, and intermolecular reaction of its β-lactam and formimidoyl groups, forming 2 and 8 separately and 8 and 10 together (Scheme II). Reactions involving carboxylic acid groups, important at lower pH values, are insignificant at pH 9 where they are largely deprotonated. Also, the pH–stability profile of dilute 1 indicates that hydrogen ion-catalyzed hydrolysis and spontaneous degradation of the β-lactam group are insignificant compared with hydroxide ion-catalyzed hydrolysis at pH 9 (eq. 1).

A kinetic model of the decomposition in weakly alkaline solution was constructed of simultaneous differential equations describing the derivatives of the molarities of 1, 2, and 8–11. Intermolecular reactions of β-lactam and formimidoyl groups were modeled as second order. The reactivity of 1 with 2-methoxyethylamine was found proportional to the fraction of amine that was unprotonated. Thus, the concentrations of the unprotonated forms of the formimidoyl reactants 1 and 10, calculated using the pK_a value of 9.9 for 1, appeared in the rate expressions of the model.

β-Lactam hydrolyses of 1 and 8 were modeled as pseudo first order. Compound 8 formed in dilute 1 solutions at pH 8 to 9.5 in amounts indicating stronger pH dependence of formimidoyl hydrolysis compared with β-lactam hydrolysis. This behavior was expressed in the model by including the fraction of formimidoyl groups that were unprotonated as a factor in the rate expression for the formimidoyl group hydrolysis of 1, together with M_1 and M_{OH^-}. The formimidoyl group hydrolyses of 2 and 10 were handled similarly, using the pK_a for 1.

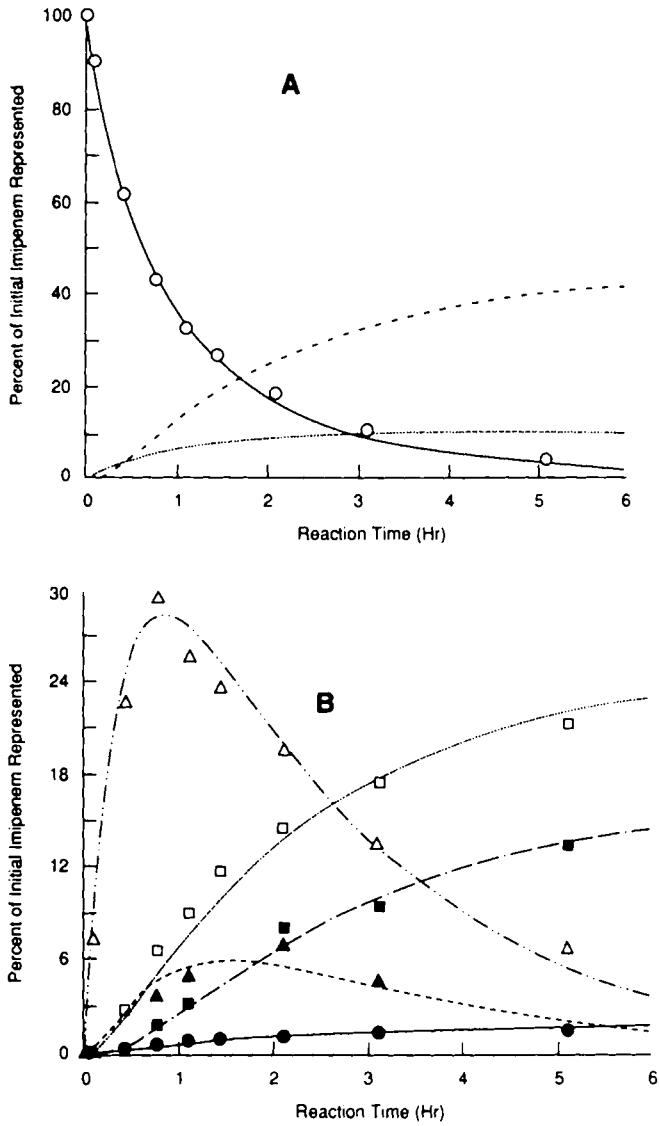

Figure 3—(**A**) Decomposition at pH 4.0 with initial 1 concentration of 20 mg/mL. Key: (○) 1 data; (——) 1 calculated; (------) 2 calculated; (– – – –) pool calculated. (**B**) Decomposition at pH 4.0 with initial 1 concentration of 20 mg/mL. Key: (△) 3 data; (— -- —) 3 calculated; (□) 4a data; (------) 4a calculated; (▲) 5 data; (– – – –) 5 calculated; (■) 6 data; (– — · –) 6 calculated; (●) 7 data; (——) 7 calculated.

The kinetic data included HPLC peaks of 1, 8, 10, and 11 that were separated on a PLRP-S column monitored at 295 nm, the wavelength at which all of the peaks were measured with limits of detection of <0.1% of the initial peak area of 1. Kinetic data were not obtained for 2 and 9, which eluted at the solvent front. Chromatograms of pH 9.0–9.5 reaction mix-

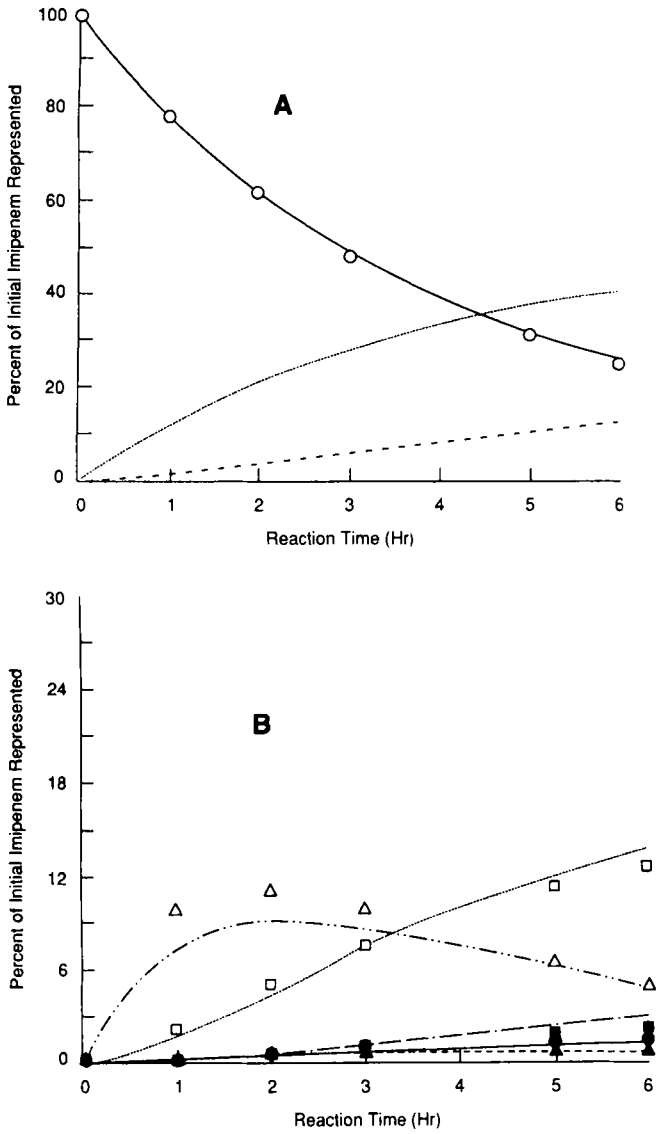

Figure 4—**(A)** Decomposition at pH 4.0 with initial **1** concentration of 2 mg/mL. Key: (○) **1** data; (——) **1** calculated; (------) **2** calculated; (– – – –) pool calculated. **(B)** Decomposition at pH 4.0 with initial **1** concentration of 2 mg/mL. Key: (△) **3** data; (— -- —) **3** calculated; (□) **4a** data; (------) **4a** calculated; (▲) **5** data; (– – – –) **5** calculated; (■) **6** data; (– — - –) **6** calculated; (●) **7** data; (——) **7** calculated.

tures monitored at several wavelengths had revealed no other peaks.

The model extended beyond the most important steps, shown in Scheme II, to include intermolecular reactions of the β-lactam groups of 1 and 8 with the formimidoyl group of 2 and with the amino groups of 8, 9, and 11. Mole percent of initial 1 represented in another "pool" of products of these reactions was calculated. (The pK_a value 8.6 of 8, available in our laboratory,[9] was used to calculate the fraction of amino reactants that were unprotonated.)

The model was fitted to data from three kinetic runs at 20 °C; two runs at pH 9.0 with initial 1 concentrations of 20 and 2 mg/mL, and one run at pH 9.5 with the higher concentration. Sodium chloride was included in the reaction mixture of the lower concentration run to make the ionic strengths equal. In another run at pH 9.0 and 2 mg/mL without sodium chloride, however, no ionic strength effect was evident. The simultaneous differential equations were integrated to obtain molarities and the "pool" content as functions of reaction time, and area percent yields were calculated as described above. A response factor of unity was used for 8, whose UV spectrum is similar to that of 1. The response factors of the dihydropyrroles 10 and 11 were assumed equal, and even though the response of 10 was known, the dihydropyrrole response factor was treated as a model parameter. Rate constants for the several reaction steps in Scheme II were calculated as separate parameters. Equal reactivities of like functional groups were assumed only in calculating the "pool" content. The model parameters were adjusted to minimize the aggregate sum of squared residuals of 1, 8, 10, and 11 in the three kinetic runs.

When the iterative adjustment was made from various starting parameter values, the final calculated curves were found essentially invariant. Rate constants for 1 β-lactam group and 1 formimidoyl group hydrolyses and for the intermolecular reaction of those 1 groups were determined, since those final values were independent of the starting values (Table III). The other rate constants were shown to be ambiguous in that their final values depended on the starting values. The calculated dihydropyrrole response factor was independent of the starting values and agreed with the known response of 10.

The results for the kinetic runs at pH 9.0 and 9.5 are plotted in Figures 5, 6, and 7. The data and fitted concentration curves of 1 are shown in Figures 5A, 6A, and 7A along with the corresponding calculated curves of 2, 9, and the "pool", defined implicitly. The data and fitted curves of the explicit degradates are shown in Figures 5B, 6B, and 7B. (The initial 8 value indicates 0.5% impurity in the starting material. Compounds 1 and 8 coeluted in the other HPLC system used for the studies at pH 4, a pH at which 8 is not a degradate.) The ordinate of each curve is scaled to indicate the percentage of initial 1 represented. At higher concentrations, 1 is less stable because of its second-order intermolecular reactivity. Both the intermolecular reactions and the formimidoyl group hydrolyses are favored at higher pH (i.e., with larger fractions of formimidoyl groups unprotonated).

Conclusions

Decomposition of aqueous 1 in the neutral pH range was investigated by means of kinetic studies of weakly acidic and weakly basic solutions. Two kinetic models of considerable complexity, encompassing our understanding of the decomposition, were constructed and fitted to the HPLC data.

Limitations both of the data and the models were obvious. Some decomposition products were not observed and their implicit concentrations could only be calculated. Some rate constants of both models were found ambiguous. Even so, the rates of all the reactions contributing to the initial decomposition were clearly defined. These reactions include a hydrogen ion-catalyzed hydrolysis and an intermolecular reaction that are important in weakly acidic solution, hydroxide ion-catalyzed hydrolyses and another intermolecular reaction that are important in weakly basic solution, and spontaneous degradation of the β-lactam group that is significant relative to the other reactions only near pH 7.

Initial disappearance rates of 1 in the neutral pH range were fully accountable in terms of the calculated rates of those reactions (Table III). Initial 20 °C rate–pH profiles, calculated using the model rate expressions and fitted rate constants for 1 concentrations of 20 and 2 mg/mL, are shown in Figure 8 along with the initial rate data. The profile calculated for zero concentration (infinite dilution) is included also. The calculated curves agree with the rates at 20 °C, measured in the present study for solutions in MES and MOPS buffers at pH 5 to 8, and with rates at 25 and 40 °C, measured previously[1] and extrapolated to 20 °C using the Arrhenius equation.

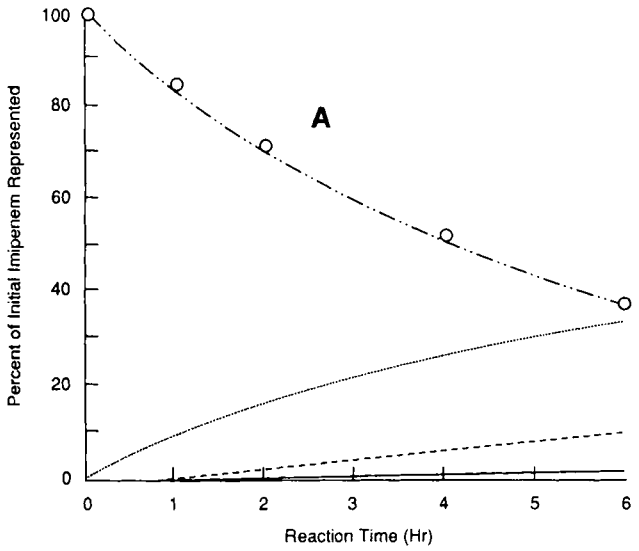

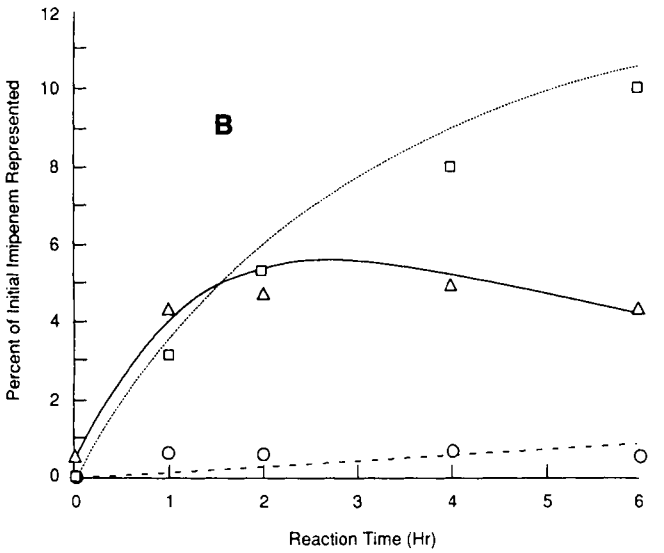

Figure 5—(A) Decomposition at pH 9.0 with initial **1** concentration of 20 mg/mL. Key: (○) **1** data; (— -- —) **1** calculated; (------) **2** calculated; (——) **9** calculated; (– – – –) pool calculated. (**B**) Decomposition at pH 9.0 with initial **1** concentration of 20 mg/mL. Key: (△) **8** data; (——) **8** calculated; (□) **10** data; (------) **10** calculated; (○) **11** data; (– – – –) **11** calculated.

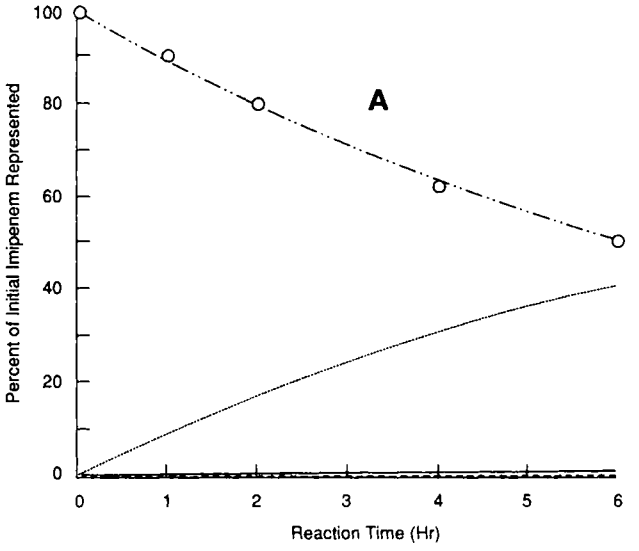

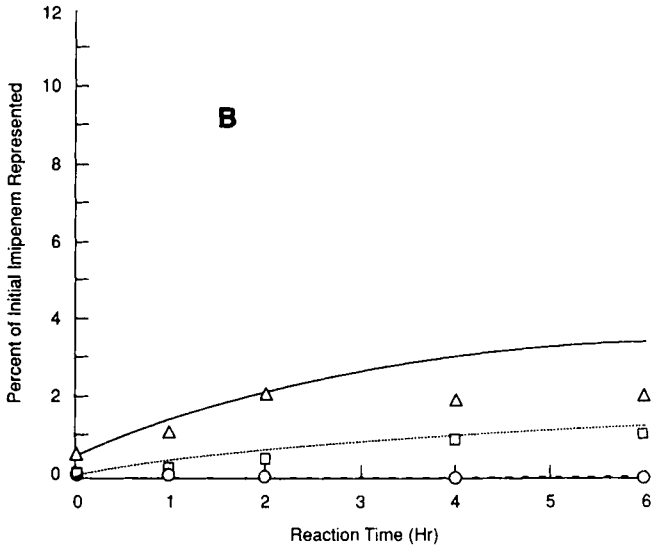

Figure 6—(A) Decomposition at pH 9.0 with initial **1** concentration of 2 mg/mL. Key: (○) **1** data; (— -- —) **1** calculated; (------) **2** calculated; (——) **9** calculated; (– – – –) pool calculated. (**B**) Decomposition at pH 9.0 with initial **1** concentration of 2 mg/mL. Key: (△) **8** data; (——) **8** calculated; (□) **10** data; (------)**10** calculated; (○) **11** data; (– – – –) **11** calculated.

Apparently, all of the significant initial reactions had been taken into account.

Experimental Section

Materials—Acetonitrile (Fisher HPLC-grade), potassium phosphate monobasic (Fisher certified ACS), and sodium hydroxide solution 50% (w/w; Fisher certified) were used to prepare HPLC mobile phases. Formamidine acetate, MES [2-(*N*-morpholino)ethanesulfonic acid] hydrate, MOPS [3-(*N*-morpholino)propanesulfonic acid], and 2-methoxyethylamine were Aldrich 99% pure materials. Sodium acetate and sodium chloride (Fisher certified ACS) and acetic acid glacial and sulfuric acid (Fisher reagent ACS) were used.

Imipenem (**1**) was obtained from the Merck Chemical Manufacturing Division. An aqueous 0.1 M solution of the *S*-methyl analogue of **1**[4] was adjusted to pH 3 with sulfuric acid to precipitate the model diketopiperazine **4b**. The precipitate was extracted into methylene chloride which was evaporated, and the residue was triturated with ethyl ether, dried, and used without further purification. Compounds **4a**, **7**, and **10** were isolated using HPLC and characterized by NMR. The NMR data for **4a** and **4b** are reported elsewhere.[4] Doubling of a number of ^{13}C signals and of key ^{1}H patterns of **7** revealed its asymmetric nature. Proton and ^{13}C assignments for **7** and **10** are shown in Tables IV and V, referring to the numbering on the structures shown. Assignments were made consistent with two-dimensional "COSY" proton correlation spectra and "APT" ^{13}C spectra. Chemical shifts are referenced only to the spectrometer operating frequency, which is based in turn on the D_2O lock frequency.

Compound **10** was the major reaction product of an aqueous solution of 0.03 M **1** and 0.25 M formamidine acetate, aged 4 h under

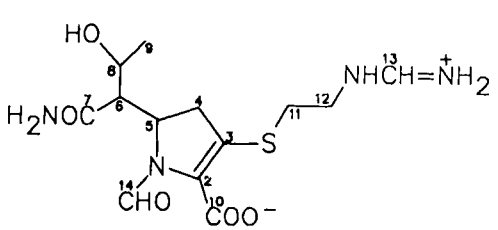

10

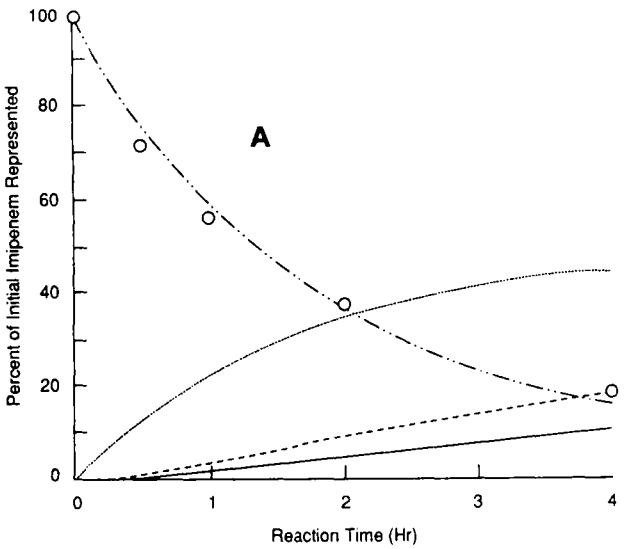

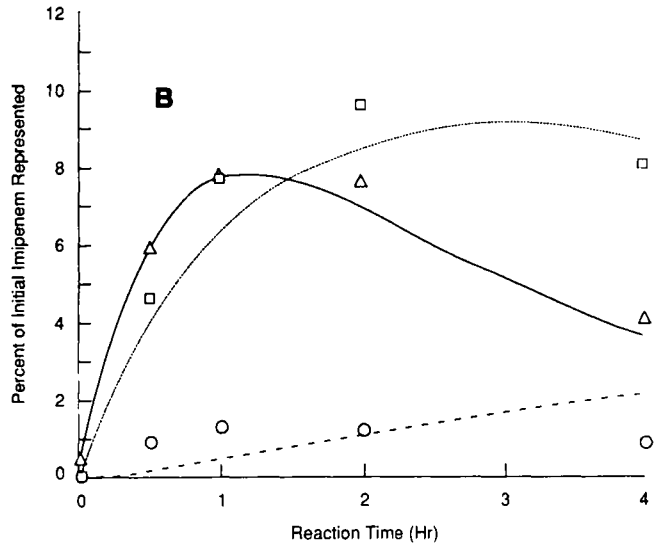

Figure 7—(A) Decomposition at pH 9.5 with initial **1** concentration of 20 mg/mL. Key: (○) **1** data; (— -- —) **1** calculated; (------) **2** calculated; (——) **9** calculated; (– — – —) pool calculated. **(B)** Decomposition at pH 9.5 with initial **1** concentration of 20 mg/mL. Key: (△) **8** data; (——) **8** calculated; (□) **10** data; (------)**10** calculated; (○) **11** data; (– — – —) **11** calculated.

nitrogen at pH 8 and 45 °C. The solution was added to a polymeric absorbent resin (Mitsubishi SP-207) and eluted with methanol:water (20:80, v/v). The fraction containing **10**, detected by its absorbance at 290 nm, was evaporated to dryness and recrystallized as a monohydrate from acetone:water. The water of hydration was evident in the FTIR spectrum; weight loss of 5.3% was found by thermogravimetry (calc. 5.23%); MS: *m/e* = 344 by fast atom bombardment.

Anal.—Calc. for $C_{13}H_{20}N_4O_8S \cdot H_2O$: C, 43.09; H, 6.12; N, 15.46. Found: C, 42.77; H, 6.08; N, 15.13.

Kinetic Runs—Aqueous 0.25, 0.5, and 1 M MES buffers (pK_a = 6.15), with and without added sodium chloride, were adjusted to pH 5 and 6 with concentrated aqueous sodium hydroxide. The MOPS buffers (pK_a = 7.2), pH 7 and 8, were prepared similarly. Solutions of **1** [0.06 and 0.006 M (20 and 2 mg/mL)] in the buffers were kept at 20 or 25 °C under nitrogen. Aliquots were analyzed periodically for intact β-lactam groups using the UV assay described previously[1] or for unreacted **1** using HPLC, see below. The MES and MOPS buffer solutions of **1** (0.005 M), at several pH values from 4.5 to 8.5 and containing 2-methoxyethylamine or sodium acetate (0.5 or 1.0 M), were kept at 25 °C under nitrogen and analyzed periodically using the UV assay.

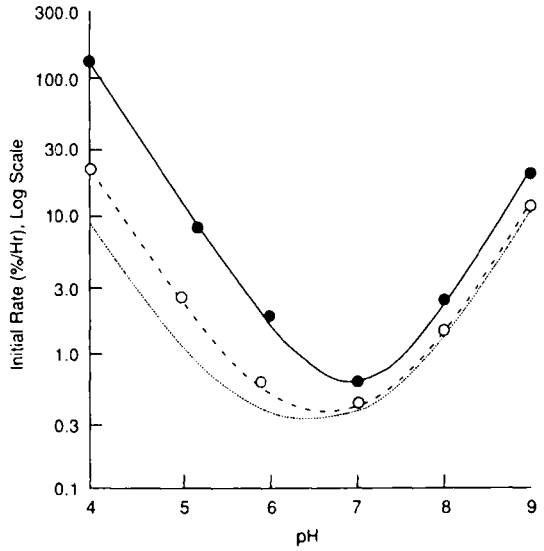

Figure 8—Stability profiles of imipenem (**1**) at 20 °C. Key: (——) 20 mg/mL, calculated; (●) 20 mg/mL, data; (– — – —) 2 mg/mL, calculated; (○) 2 mg/mL, data; (------) 0 mg/mL, calculated.

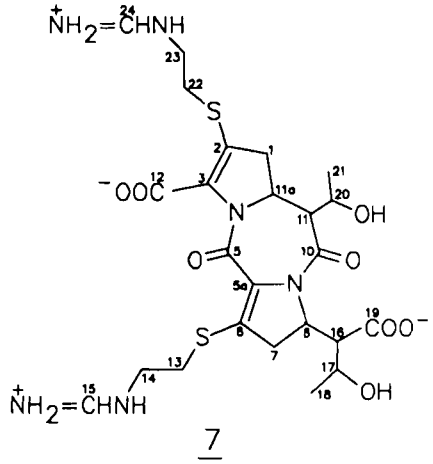

7

Table IV—Nuclear Magnetic Resonance Data for Compound 7

Position	^{13}C	^{1}H
1, 7[a]	37.3, 38.8	2.9–3.4(m)
2	—[b]	—
3	—[b]	—
5, 10[a]	158.5, 159.0	—
5a	—[b]	—
6	—[b]	—
8	59.0	5.17(dd), *J* = 8.1, 3.7
11	50.9	3.30(dd), *J* = 9.9, 3.9
11a	61.9 or 62.9[c]	4.59(ddd), *J* ~10, ~10, 8.6
12	173.2	—
13, 22[a]	29.8, 30.7[d]	2.9–3.4(m)
14, 23[a]	41.9, 42.0[d]	3.5–3.8(m)
15, 24[a]	155.4, 155.6[d]	7.86±[d]
16	61.9 or 62.9[c]	2.30(dd), *J* = 10.2, 3.7
17	67.1	3.91(dq), *J* = 10.2, 6.2
18	21.1	1.21(q), *J* = 6.2
19	178.6	—
20	67.1	4.31(dq), *J* = 3.8, 6.7
21	19.4	1.49(q), *J* = 6.7

[a] Assignments may be interchanged. [b] Assignment uncertain due to limited S/N. [c] ^{13}C assignments may be interchanged. [d] Only signals to major components of *Z*- and *E*-formamidinium isomeric equilibria listed.

Table V—Nuclear Magnetic Resonance Data for Compound 10

Position	^{13}C[a]	^{1}H
2	133.3/not observed	—
3	129.5/128.9	—
4	37.2⁻/37.2⁺	2.90(dd), J = 17.2,2.0 3.29(dd), J = 17.2,9.8
5	55.3	4.99(dt)
6	59.7	2.44(dd), J = 10.2,3.4
7	176.2/176.1	—
8	66.1	3.98(dq), J = 10.2,6.3
9	20.8	1.22(d), J = 6.2
10	167.2	—
11	29.7/31.9	3.09(m)
12	47.4/42.0	3.57(m)
13	155.4/158.5[b]	7.85(s)/7.81(s)[a]
14	165.1[c]	8.82(s)

[a] Shifts are given for *Z*- and *E*-formamidinium isomers where distinguishable. [b] $^{1}J_{13CH}$ = 194 Hz(*Z*), 193 Hz(*E*). [c] $^{1}J_{13CH}$ = 206.1 Hz.

Aqueous solutions of 1 (0.06 or 0.006 M), with sodium chloride in the latter to make the ionic strengths equal, were initially adjusted to pH 4.0 with sulfuric acid and the pH remained constant. Other such solutions were maintained at pH 9.0 or 9.5 using a pH stat to control addition of aqueous sodium hydroxide. These unbuffered solutions were kept at 20 °C under nitrogen and were analyzed periodically for 1 and several degradates using HPLC. The D_2O solutions of 1 (0.06 M) under nitrogen were adjusted initially to pD 4.0 with sulfuric acid and analyzed using NMR and FTIR. Occasionally, aliquots were adjusted to pH ~1 with sulfuric acid or were made 0.5 M in hydroxylamine (pH ~8). After aging briefly at room temperature, these aliquots were analyzed using HPLC.

High-Performance Liquid Chromatography Methods—Liquid chromatography was performed using an HPLC system composed of LDC Constametric I and II pumps and Gradient Master, a Spectra Physics (Schoeffel) model 770 spectrophotometric detector and SP4100 computing integrator, and a Hewlett-Packard model 1040A diode array detector.

A 250 × 4.6-mm Partisil PXS 5/25 PAC column (Whatman) was used for kinetic runs at pH 4. The acetonitrile:water mobile phase was delivered at a rate of 2 mL/min as a linear gradient from 25 to 50% water in 30 min, with the column at ambient temperature (~23 °C), and the effluent was monitored at 320 nm. Degradates were isolated for spectroscopic examination using a M9 Partisil 10/50 PAC column.

A 150 × 4.6-mm PLRP-S styrene-divinylbenzene copolymer column (Polymer Labs) was used for kinetic runs at pH > 4 and for degradate isolation. The mobile phase, composed of 0.02 M KH_2PO_4-NaOH pH 7.2 buffer and acetonitrile, was delivered at a rate of 1.2 mL/min as a linear gradient from 3 to 7% acetonitrile in 22 min with the column at 40 °C, and the effluent was monitored at 295 nm.

References and Notes

1. Smith, G. B.; Schoenewaldt, E. F. *J. Pharm. Sci.* **1981**, *70*, 272–276.
2. *CRC Handbook of Chemistry and Physics,* 66th ed.; CRC: Boca Raton, FL, 1985; p D-161.
3. Lotz, J. R. *J. Phys. Chem.* **1959**, *63*, 541–554.
4. Ratcliffe, Ronald W.; Wildonger, Kenneth J.; DiMichele, Lisa; Douglas, Alan W.; Hajdu, Richard; Goegelman, Robert T.; Springer, James P.; Hirschfield, Jordan *J. Org. Chem.* **1989**, *54*, 653–660.
5. Kahan, J. S.; Kahan, F. M.; Goegelman, R.; Currie, S. A.; Jackson, M.; Stapley, E. O.; Miller, T. W.; Miller, A. K.; Hendlin, D.; Mochales, S.; Hernandez, S.; Woodruff, H. B.; Birnbaum, J. *J. Antibiot.* **1979**, *32*, 1–12.
6. *Dissociation Constants of Organic Acids in Aqueous Solution;* Kortum, G.; Vogel, W.; Andrussow, K., Eds.; Butterworths: Washington, DC, 1961; p 309.
7. Gear, C. William *Numerical Initial Value Problems in Ordinary Differential Equations;* Prentice-Hall: Inglewood Cliffs, NJ, 1971.
8. Nelder, J. A.; Mead, R. *Computer J.* **1965**, *7*, 308–313.
9. McCauley, J. A., personal communication.

Acknowledgments

This study was accomplished through teamwork involving many Merck employees. The authors thank especially Dr. R. W. Ratcliffe for preparing the diketopiperazine 4b, Dr. F. E. Roberts for isolating the dihydropyrrole 10, Mr. R. A. Reamer and Ms. L. DiMichele for NMR, Dr. S. M. Riseman for FTIR, Mr. J. L. Smith for MS, Dr. J. A. McCauley for thermogravimetry, Dr. A. K. Majumdar for computer programming assistance and implementation of simplex optimization, and Miss M. T. Spears for typing the manuscript.